tarjomehrooz.com 0902 795 28 76 ترجمه تخصصی توسط دکتری رشته مربوطه و برای کلیه زبان های خارجی + شبیه سازی مقالات با کلیه نرم افزار ها مشاوره گمرکی و...

Applied Energy 159 (2015) 285–297

Contents lists available at ScienceDirect

Applied Energy

journal homepage: www.elsevier.com/locate/apenergy

A novel multistage Support Vector Machine based approach for Li ion battery remaining useful life estimation

Meru A. Patil [a], Piyush Tagade [a], Krishnan S. Hariharan [a,*], Subramanya M. Kolake [a], Taewon Song [b], Taejung Yeo [b], Seokgwang Doo [b]

[a] Computational Simulations Group (SAIT-India), Samsung R&D Institute India-Bangalore, #2870 Phoenix Building, Bagmane Constellation Business Park, Outer Ring Road, Doddanekundi Circle, Marathahalli Post, Bangalore 560 037, India
[b] Energy Material Lab, SAIT, Samsung Electronics, Gyeonggi-do 443-803, Republic of Korea

HIGHLIGHTS

- Novel multi step data analytic approach combining classification and regression.
- Extraction of minimal set of critical features from battery cycling data.
- Validation based on open source data of various types of batteries.
- Accurate and fast estimation of RUL of multi-cell data.

ARTICLE INFO

Article history:
Received 17 June 2015
Received in revised form 10 August 2015
Accepted 22 August 2015

Keywords:
Remaining Useful Life
Classification
Regression
Support Vector Machine
Battery life models

ABSTRACT

Real-time prediction of remaining useful life (RUL) is an essential feature of a robust battery management system (BMS). In this work, a novel method for real-time RUL estimation of Li ion batteries is proposed that integrates classification and regression attributes of Support Vector (SV) based machine learning technique. Cycling data of Li-ion batteries under different operating conditions are analyzed, and the critical features are extracted from the voltage and temperature profiles. The classification and regression models for RUL are built based on the critical features using Support Vector Machine (SVM). The classification model provides a gross estimation, and the Support Vector Regression (SVR) is used to predict the accurate RUL if the battery is close to the end of life (EOL). By the critical feature extraction and the multistage approach, accurate RUL prediction of multiple batteries is accomplished simultaneously, making the proposed method generic in nature. In addition to accuracy, the multistage approach results in faster computations, and hence a trained model can potentially be used for real-time onboard RUL estimation for electric vehicle battery packs.

© 2015 Elsevier Ltd. All rights reserved.

1. Introduction

Ongoing energy crisis and environmental concerns are driving rapid modifications in the electric vehicle (EV) technologies [1–3]. The EVs are expected to aggressively penetrate the transportation market, with US predicted to have one million EVs on road by 2015 and China to have five million EVs by 2020 [4]. Driving range and reliable operation under various drive cycles, however, are the major concerns for EVs that use the current state of art technologies for state and health diagnosis.

Battery power system plays a critical role in ensuring a long driving range of the EV, along with the reliable operation under various driving scenarios like turn and acceleration. Considering the high energy density, high cell voltage, low self-discharge and long cycle life, Lithium-ion (Li-ion) batteries are preferred over the traditional batteries for the EVs [5–7]. Li-ion batteries however, are prone to safety issues due to operational performance deterioration. The on-board battery state and health monitoring is critical to track the available battery power and avoid catastrophic failures. Often, battery state of charge (SOC) and state of health (SOH) are monitored, which provide useful information for the battery management system (BMS). SOC estimates the remaining charge available with the battery, and thus indicates when the battery needs recharge. Various direct and indirect methods are proposed in the literature for SOC estimation [8,9]. The SOH is a measure of the health of the battery that indicates the remaining time before the battery pack needs to be replaced. Health

* Corresponding author.
E-mail address: krishnan.sh@samsung.com (K.S. Hariharan).

http://dx.doi.org/10.1016/j.apenergy.2015.08.119
0306-2619/© 2015 Elsevier Ltd. All rights reserved.

tarjomehrooz.com 0902 795 28 76 ترجمه تخصصی توسط دکتری رشته مربوطه و برای کلیه زبان های خارجی + شبیه سازی مقالات با کلیه نرم افزار ها مثلب گمز و ...

Nomenclature

BMS	battery monitoring system
Cap	capacity
CCI	concave convex index
CI	curvature index
E	energy of a signal
EOL	end of life
FI	fluctuation index
K(·,·)	Kernel for SVM/SVR
KI	kurtosis index
N	no. of sampling points
RUL	remaining useful life
SI	skewness index
SOC	state of charge
SOH	state of health
SVM	Support Vector Machine
SVR	support vector regression
t	time (s)
T	temperature (K)
V	voltage (V)

Greek letters

α, β	Lagrange multipliers
ε	misclassification error
μ	mean
ω	sampling frequency

Subscripts

max	maximum
min	minimum

monitoring of battery for EV and HEV applications is addressed using various approaches [5] and are broadly classified as diagnosis and prognosis [10]. Diagnosis pertains to tracking the degradation mechanisms and measures during the event of battery failure. Prognosis pertains to prediction of the remaining useful life (RUL). RUL is an estimate of the number of cycles the pack can be used within the limits of satisfactory performance.

Offline discharge testing and online internal resistance measurement [11] based methods are reported in literature for SOH estimation. These methods, however, require sophisticated instrumentation and rigorous testing that are often difficult for on-board implementation. Current research in SOH estimation is focused on developing computationally efficient real-time algorithms. Model based fusion approaches are extensively investigated in the literature for real time battery state estimation [5]. The fusion approaches primarily use a filtering algorithm in a closed loop format, where error between the model prediction and measurements is fed-back to correct the state. In a series of three papers, Plett [12–14] have proposed the extended Kalman Filter (EKF) for battery state estimation and demonstrated its effectiveness for quantitative SOC estimation. Subsequently, the EKF is used by several authors for battery state and parameter estimation (see, for e.g. [15–17]). In [18], EKF is used with KF in a dual filtering framework, where KF is used for SOC estimation and EKF for SOH estimation of a lead acid battery. Zou et al. [19] use two instances of EKF in a similar dual filtering framework, where EKFs with different time scales are used for combined SOC and SOH estimation. Xiong et al. [20] propose an adaptive EKF algorithm for battery state estimation and demonstrate its effectiveness for SOC estimation.

Although accurate for mildly non-linear models, the EKF requires costly Jacobian calculations and often fails in presence of high non-linearity. Sigma-Point Kalman Filters (SPKF) (also known as the unscented Kalman Filter) can address some limitations of the EKF [21]. The SPKF is used by several authors for battery state estimation, for e.g., Plett use the SPKF for SOC estimation of a Lithium polymer battery [22]. In [23], authors combine KF with SPKF to propose a dual filter, which is used for battery SOC and internal state estimations. They also calculate battery SOH from the estimated capacity.

Several other authors use a Particle Filter (PF) for battery state estimation, which is an optimal filter for a non-linear model with non-Gaussian noise [24]. In [25,26], Saha et al. use PF for SOH estimation, while in [27] the PF based framework is used to investigate the battery SOH regeneration phenomenon. Wang et al. [28] use the PF for a combined battery SOC and state of energy estimation. Liu et al. [29] use the PF with an autoregressive time series degradation model for RUL estimation. Some recent modifications to the PF algorithm are also exploited for battery state estimation, like regularized auxiliary PF in [30], unscented PF in [31] and Gauss-Hermite PF in [32]. Saha et al. [33] presents a comparative study of the different SOH estimation methods and demonstrates the comparative superiority of PF over the existing fusion methods.

Health monitoring based on machine learning tools are gaining importance for SOH estimation in recent years [34]. Prominent among these are artificial neural networks (ANN) [34–36] (reviewed in [5]) and Support Vector Machines (SVM). The SVM is one of the most popular machine learning algorithms, which is used in the pattern recognition community for classification tasks [37]. Current SOH estimation algorithms primarily use SVM as a regression tool where a variant of the algorithm, known as Support Vector Regression (SVR) [38], is implemented. Several early works use SVM for battery SOC estimation [38,39]. Klass, Behm and Lindbergh [40] use SVM for SOH estimation, where they model the cell voltage as a function of load current and SOC. The authors use SVM model in virtual tests to estimate the battery internal resistance, which is in turn used as a measure of SOH. Klass, Behm and Lindbergh further extend the work in [41] by introducing temperature dependence in the model. Battery capacity is also estimated using virtual tests, which is used as an indicator of the internal resistance and SOH. To improve the accuracy of SOH estimation, authors in [42] use a fusion approach, where the battery model trained using SVM is combined with a particle filtering framework. Other approaches [43–45] use the probabilistic flavor of the SVM, known as the Relevance Vector Machine (RVM), for the RUL estimation. In such cases the Bayesian inference for the RVM parameter estimation is used, and the resultant model is incorporated in the particle filtering framework for RUL estimation. Alternate applications of machine learning approaches for battery state estimation include particle swarm optimization [46], Gaussian process regression [47], recurrent neural fuzzy systems [48], genetic algorithm [49], sample entropy based approaches [50,51], the naive Bayes model [52,53] and other geometric approaches [54].

The machine learning approaches as discussed above have the advantage that SOC and SOH estimation can be done based on measured voltage, current and temperature signals, and hence can encompass a wide range of operating conditions [5]. The disadvantages are that the models require large amounts of data [34] resulting in longer times for computation. This problem is severe in SVM based models. Further, reported applications for battery SOH estimation invariably use SVM for regression. SVM inherently being a classification tool [8,5,10], modification to regression

tarjomehrooz.com 0902 795 28 76 ترجمه تخصصی توسط دکتری رشته مربوطه و برای کلیه زبان های خارجی + شبیه سازی مقالات با کلیه نرم افزار ها مثلب گمز و ...

problems is complicated. Due to this reason, SVM is used predominantly as an offline tool. It should be noted however, that SVM is acknowledged as a powerful machine learning tool [5,10] and unlike ANN [5,41], does not have local minima problems. As demonstrated in this paper, a significant performance improvement can be obtained if SVM is used for classification with regression. Using this multistage approach, a novel method of estimating remaining useful life of the Li-ion batteries at any given discharge cycle is proposed in this work. By this methodology, it is expected that the full potential of SVM can be realized.

The proposed method uses a two-stage process [55]; in the first stage gross RUL is estimated using classification technique and in the second stage regression technique is used to estimate the accurate RUL. In order to facilitate the classification, it is essential to identify the critical features in the cycling data that is most sensitive to the RUL [46,54]. Thus, the first novel contribution of this work is computation of unique features from battery discharge curves for efficient and accurate representation of cycling data. The principal novel contribution is the two-stage (classification–regression) approach for estimating RUL. The proposed approach reduces the input parameter set to a minimal set of critical features, and enables the regression to be much accurate, in addition to reducing the overall simulation time. Both these novel contributions have enabled analysis of multiple sets of battery data simultaneously with accurate RUL prediction.

Rest of the paper is organized as follows. In Section 2, a brief introduction of Support Vector Machines for classification and regression is presented. In Section 3, the proposed method is described in detail. Numerical results are presented in Section 4 along with discussion and the paper is summarized and concluded in Section 5.

2. Support Vector Machine for classification and regression

This section briefly introduces the SVM for classification and regression [37]. Without the loss of generality, the algorithm is presented for a two-class classification problem and subsequently the pointers are provided for its extension to the general classification and regression.

Consider a two-class classification problem with a training data set $(\boldsymbol{x}_i, \boldsymbol{y}_i; i = 1, \ldots, n)$, where $\boldsymbol{x}_i \in R^n$ and $\boldsymbol{y} \in \{-1, 1\}$. The data point can be separated using a hyperplane given by

$$\langle \omega, \boldsymbol{x} \rangle + b = 0, \tag{1}$$

where ω is a parameter vector and $\langle \cdot, \cdot \rangle$ denotes a dot product. The classification problem is to find an optimal separating hyperplane, which maximizes the distance between itself and the nearest data point of each class. The optimal separating hyperplane must satisfy the canonical constraint

$$\boldsymbol{y}_i[\langle \omega, \boldsymbol{x}_i \rangle + b] \geqslant 1 - \varepsilon_i, \tag{2}$$

where ε_i is a non-negative measure of the misclassification error. The optimal separating hyperplane is defined using

$$\Phi(\omega, \xi) = \frac{1}{2}\|\omega\|^2 + C\sum_i \xi_i, \tag{3}$$

subject to the constraint in Eq. (2). Here, C is a user defined value. The optimization problem is solved using Lagrangian multipliers, where the optimum is a saddle point of the Lagrangian

$$\Phi(\omega, b, \xi, \alpha, \beta) = \frac{1}{2}\|\omega\|^2 C\sum_i \xi_i - \sum_i \alpha_i(\boldsymbol{y}_i[\boldsymbol{\omega}^T \boldsymbol{x}_i + b] - 1 + \xi_i) - \sum_i \beta_i \xi_i, \tag{4}$$

while α and β are the Lagrange multipliers. The Lagrange multipliers are zero except for a small subset of the input vectors. This small subset is known as the support vectors (SVs) [37].

The SVM can be adapted for a regression problem using the SVR algorithm, where objective is to find an optimal function

$$f(\boldsymbol{x}) = \langle \omega, \boldsymbol{x} \rangle + b. \tag{5}$$

Goal of the SVR is to find a function (Eq. (5)) such that the maximum deviation of $f(\boldsymbol{x})$ from an arbitrary training data is less than a user defined value ε, while maintaining the highest possible flatness. The resultant optimization problem has a form

$$\Phi(\omega, \xi) = \frac{1}{2}\|\omega\|^2 + C\sum_i \xi_i, \tag{6}$$

subject to the constraints

$$\boldsymbol{y}_i - \langle \omega, \boldsymbol{x}_i \rangle - b \leqslant \varepsilon + \xi_i. \tag{7}$$

Required function is the optimal of the Lagrangian

$$\Phi(\omega, b, \xi, \alpha, \beta) = \frac{1}{2}\|\omega\|^2 + C\sum_i \xi_i - \sum_i \alpha_i([\boldsymbol{\omega}^T \boldsymbol{x}_i + b] - \boldsymbol{y}_i + \varepsilon + \xi_i) - \sum_i \beta_i \xi_i. \tag{8}$$

The resultant optimized target function has the form

$$f(\boldsymbol{x}) = \sum_{i=1}^{L} \alpha_i \langle \boldsymbol{x}_i, \boldsymbol{x} \rangle + b, \tag{9}$$

where $\boldsymbol{x}_i$ are the support vectors.

The main advantage of the SVM algorithm for classification and regression is the final formulation in terms of the support vectors, which condenses the large training data to a significantly smaller subspace of SVs. Moreover, the formulation does not require any computationally intensive mathematical operations. The proposed method exploits these advantages of the SVM to obtain a computationally efficient RUL estimation algorithm.

3. Proposed methodology

The objective of this work is to design an efficient two-stage RUL estimation system that can predict the remaining life of a battery at any stage of its life. Fig. 1 provides the block diagram of this methodology. The motivations behind design of such a two-stage system are twofold:

(a) For on-board scenarios, accurate RUL estimation is required only when the battery is close to end of life as against fresh.
(b) Addition of a classification step before the regression step eliminates the need to perform regression across the complete battery life cycle data. Hence due to introduction of this step, heavy computations can be eliminated.

This section provides a detailed description of the proposed methodology used in development of classification and regression models. In Section 3.1, data formatting and processing is explained and Section 3.2 describes the development of classification model. Finally in Section 3.3, the regression model development is described in detail.

3.1. Data processing and feature extraction

In this work, data collected from discharge cycles of Li-ion batteries cycled under various conditions are analyzed. The battery cycling data is sourced from a publically available repository; provided by Prognostics Center of Excellence (PCoE) at Ames Research Center, NASA [56]. Table 1 lists the 19 batteries used in this work, along with their respective operating parameters. The data repository [56] contains capacity, voltage, current, temperature, current load and voltage load recorded for each discharge cycle of the

tarjomehrooz.com 0902 795 28 76 ترجمه تخصصی توسط دکتری رشته مربوطه و برای کلیه زبان های خارجی + شبیه سازی مقالات با کلیه نرم افزار ها مشاوره گمرکی و ...

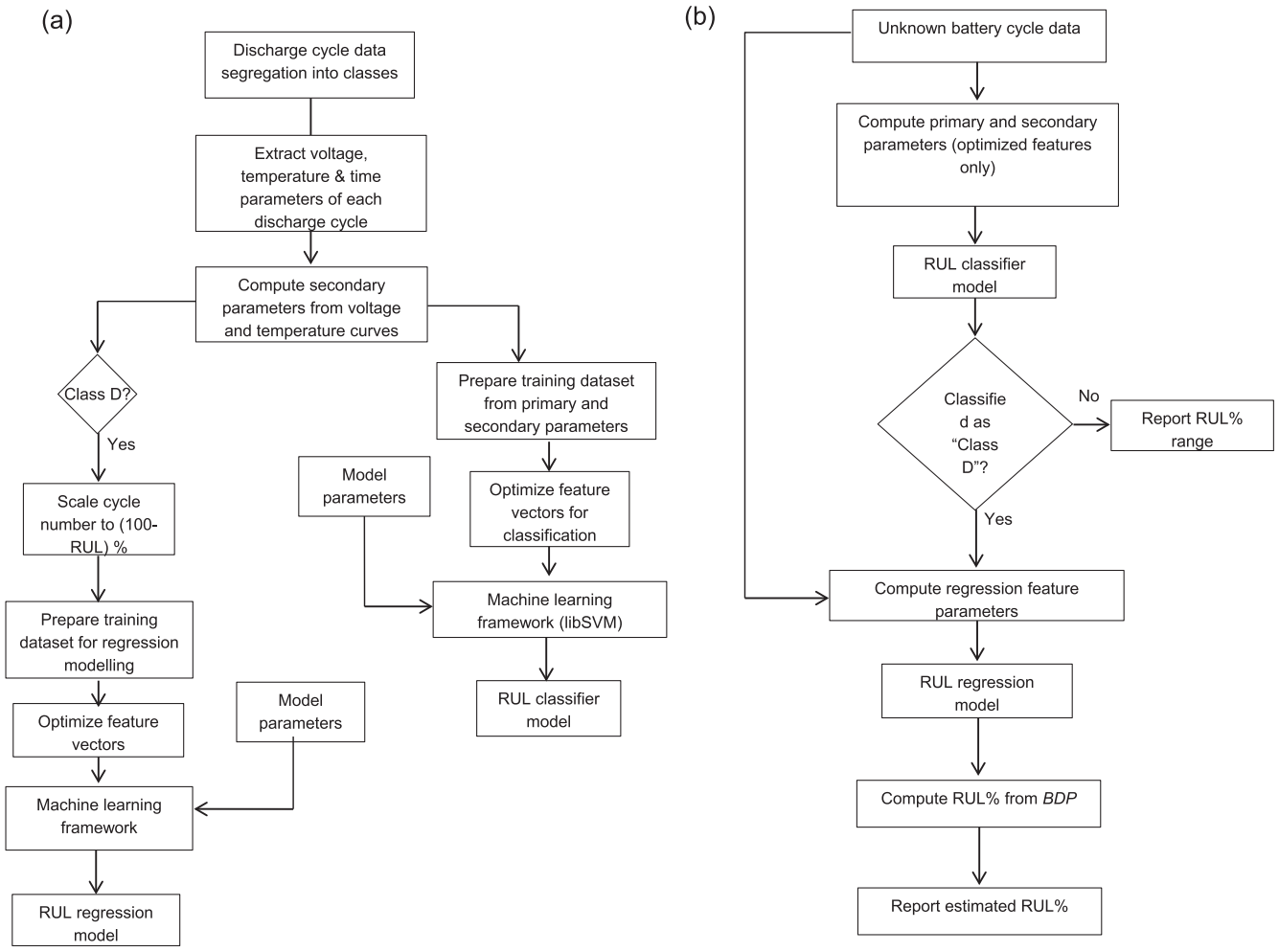

Fig. 1. (a) Flow chart for training classification and regression models. (b) Flow chart for using classification and regression models.

batteries. Except the cell capacity, all other parameters are recorded over time during discharge; however these parameters are acquired with non-uniform sampling rate. It is observed that as battery ages there will be change in measured voltage, current and temperature. Hence it is paramount to extract the relevant features [46,54] from these curves that are crucial in determining battery life. From each discharge cycle, a set of 8 parameters is extracted from voltage and temperature curves representing minimum and maximum values of each curve, and their respective times. In addition to above parameters, following 13 parameters are computed from voltage, temperature and current curves for each discharge cycle.

- **Capacity** (Cap): The capacity of battery is computed by integrating discharge current over time and it is given by:

$$\text{Cap} = \int_{t_1}^{t_2} I dt \tag{10}$$

where t_1 and t_2 are start and end time of a discharge cycle.

- **Energy of signal** (E): Signal energy of voltage and temperature curves are computed. In general, energy of signal is defined as the measure of signal strength over time and it is given by Eq. (11) below:

$$E = \int_{-\infty}^{\infty} |x(t)|^2 dt \tag{11}$$

where $x(t)$ is the signal (either voltage or temperature) and t is time. In this work *VCE* notation is used to denote energy of voltage curve and *TCE* to denote energy of temperature curve.

- **Fluctuation index of signal** (FI): Fluctuation Index of signal is defined as a measure of deviation of the signal from the mean and is given as:

$$\text{FI} = \frac{\sqrt{\sum (y_i - \mu)^2}}{\omega} \tag{12}$$

where y_i is the signal, μ is mean of the signal and ω is sampling frequency.

Curvature index of signal (CI): Defined as a measure of direction in which the unit tangent vector rotates as a function of the parameter along the signal and it is given by equation:

$$\text{CI} = \frac{\sum \theta}{N} \tag{13}$$

where $\theta = \frac{y''}{(1+y'^2)^{\frac{3}{2}}}$, and N is length of the signal.V_{CI} denotes the curvature index of voltage curve and *T_CI* denotes the corresponding curvature index of temperature curve.

- **Concave convex index** (CCI): It is a measure of convexity of the signal. A convex signal will have index >0.5 whereas a concave signal will have index <0.5. The index is calculated using slope and intersection estimation. This index is given by:

$$\text{CCI} = \begin{cases} 1 & \text{if } y_i \text{ is convex} \\ 0 & \text{if } y_i \text{ is concave} \end{cases} \tag{14}$$

tarjomehrooz.com 0902 795 28 76 ترجمه تخصصی توسط دکتری رشته مربوطه و برای کلیه زبان های خارجی + شبیه سازی مقالات با کلیه نرم افزار ها مثلب گمز و ...

Table 1
List of batteries with their operating parameters.

Battery number	Discharge current	End voltage (V)	End-of-life condition	Operating temperature (°C)	No of cycles
B0005	2 A constant current	2.7	30% fade in rated capacity (2–1.4 A h)	24	168
B0006		2.5			168
B0007		2.2			168
B0033	4 A	2.0	Capacity reduced to 20% fade (1.6 A h)	24	197
B0034		2.2			197
B0036	2 A	2.7			197
B0038	Multiple –1 A, 2 A and 4 A	2.2	Capacity reduced to 20% fade (1.6 A h)	24 & 44	47
B0039		2.5			47
B0040		2.7			47
B0042	Multiple – 1 A, 4 A	2.2	Capacity reduced to 30% fade (1.4 A h)	4	112
B0043		2.5			112
B0044		2.7			112
B0045	Fixed load – 1 A	2	Capacity reduced to 30% fade (1.4 A h)	4	72
B0046		2.2			72
B0047		2.5			72
B0048		2.7			72
B0054	Fixed load – 2 A	2.2	Capacity reduced to 30% fade (1.4 A h)	4	103
B0055		2.5			102
B0056		2.7			102

In this work voltage curve concave convex index (*VC_CCI*) and temperature curve concave convex index (*TC_CCI*) are computed.

- **Skewness index** (SI): Skewness Index is a measure of the extent to which a probability distribution of signal leans toward mean of the signal. This index is given by:

$$\mathrm{SI} = \frac{\sum_{i=1}^{n}(y_i - \mu)^3}{\sigma^3} \tag{15}$$

where y_i is input signal μ is mean of the signal and σ is standard deviation of the signal and n is length of signal. Skewness index of voltage curve is denoted by *VC_SI* and that of temperature curve is denoted by *TC_SI*.

- **Kurtosis index** (KI): It is measure of the "peakedness" of the probability distribution of the signal and it is given by the equation:

$$\mathrm{KI} = \frac{\sum_{i=1}^{n}(y_i - \mu)^4}{\sigma^4}. \tag{16}$$

VC_KI and *TC_KI* notations used to denote kurtosis index of voltage and temperature curves respectively. Fig. 2(a)–(d) depicts variation of all these features across discharge cycles for battery B0036.

3.2. Classification model

In this section, design of classification model is described in detail. Classification model is built using the features of discharge cycles computed in Section 3.1. The weka toolbox [57] along with libSVM package [58] is used in this step. Prototyping and final implementation is done using MATLAB®. For each battery, total number of discharge cycles are counted till it reaches EOL and each discharge cycle is classified into four categories, namely class *A*, *B*, *C* and *D*. This classification is done based on number of cycles it has already completed. For example, battery B0005 has completed total 168 discharge cycles to reach EOL (refer Table 1), hence first 42 discharge cycles are classified into class *A*, next 42 discharge cycles into class *B* and so on. In case if total number of discharge cycle is odd then some of the classes will get additional cycle.

Set of batteries listed in Table 1 are selected and their parametric data is aggregated and made compatible with weka toolbox. This data is heterogeneous, as it is sourced from different batteries that have operated under varying temperature, current, voltage and load conditions. Hence it is very important to analyze this data to find optimal set of features for classification. Having optimal set of features helps in enhancing accuracy of classification as well as in reducing computational time of over-all process. Principal Component Analysis (PCA) is used to extract critical parameters that represent majority of datasets. The data is further analyzed using a visualization technique. In this technique, data is plotted against two parameters (representing two axis of plot) and sensitivity of the data scatter against each parameter is investigated. Parameters with least sensitivity are neglected to obtain a critical set of parameters. For example in Fig. 3, it can be observed that a scatter plot of *Cap* v/s t_{maxT} is same as scatter plot *Cap* v/s t_{minV}. This implies that both t_{maxT} and t_{minV} vary in same way with respect to capacity. This methodology is used to find list of features that are independent of each other and contribute in optimal classification. To further optimize the classification outcome, the model parameters are tuned. Various parameters, like kernel type, cost function, allowed degree of freedom, allowed error rate and gamma value are altered to enhance accuracy of the classification. Once the values are fixed, the same values are used in final MATLAB implementation. The flow chart of training classification model is described in Fig. 1a.

3.3. Regression model

The regression model is used for accurate RUL estimation of the battery data classified as "class D". For a cell at N_i cycles, RUL is defined as:

$$\mathrm{RUL} = \frac{N_{EOL} - N_i}{N_{EOL}} \times 100 \tag{16}$$

The first step of constructing regression model is to prepare the dataset. Dataset preparation involves segregation of parametric data of the batteries considered for model creation (refer Fig. 1a). Once the data is segregated for each battery, discharge cycles belonging to "class D" are scaled. A MATLAB model based on SVR is developed for accurate regression. Various kernels like the Gaussian, exponential, hyperbolic, Wavelet, and multi-layer perceptron (MLP), were assessed for the best performance. Models are tuned by changing kernel type and optimizer parameters, and it was observed that a multi-layer perceptron (MLP) based kernel, as given in Eq. (17), gives the most reliable results.

$$K(x_i, x_j) = \tanh\left(-\frac{\lambda_{i,j}}{2\sigma^2}\right) \tag{17}$$

tarjomehrooz.com 0902 795 28 76 ترجمه تخصصی توسط دکتری رشته مربوطه و برای کلیه زبان های خارجی + شبیه سازی مقالات با کلیه نرم افزار ها مثلب گمز و ...

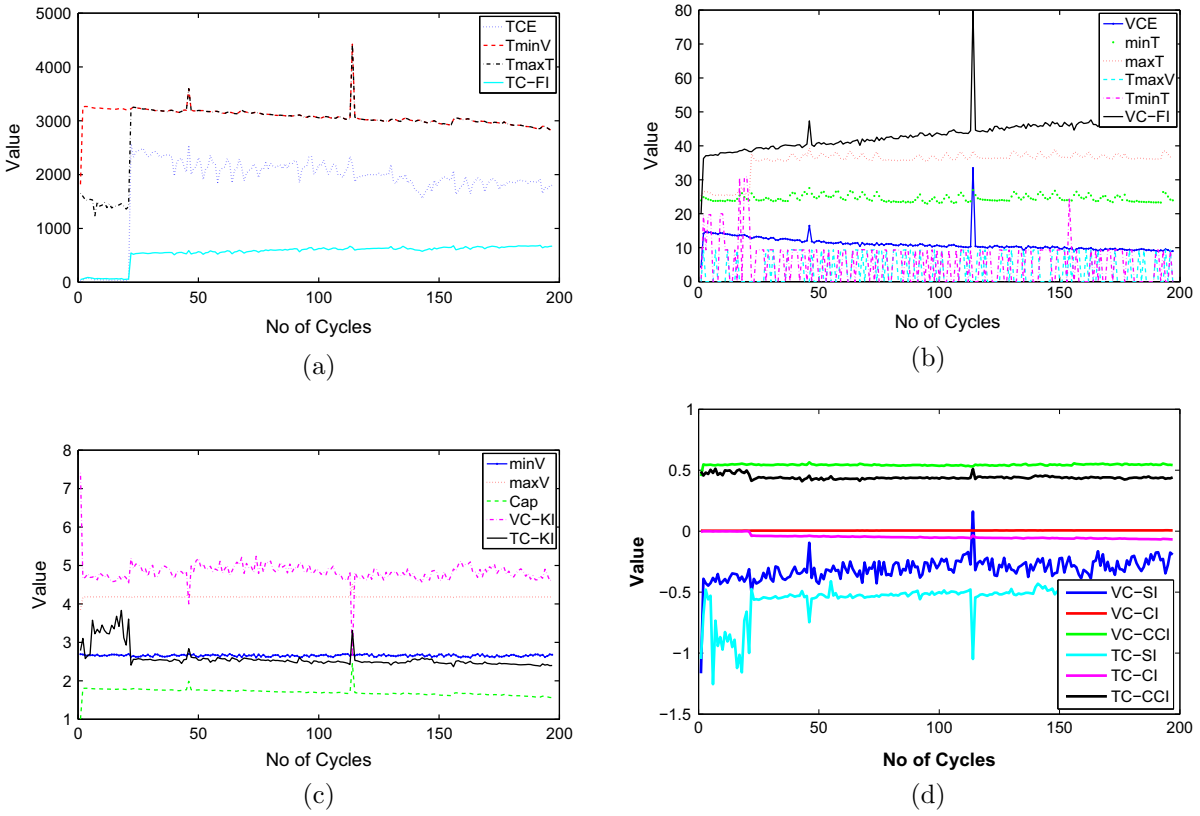

Fig. 2. Sub-figures (a)–(d) depicts all feature parameters computed for battery B0036 across its discharge cycle. (a) Parameters: *TCE*, t_{minV}, t_{maxT}, *TC_FI*. (b) Parameters: *VCE*, T_{min}, T_{max}, *TmaxV*, *TminT*, *VC_FI*. (c) Parameters: *minV*, *maxV*, *Cap*, *VC_KI*, *TC_KI*. (d) Parameters: *VC_SI*, *VC_CI*, *VC_CCI*, *TC_SI*, *TC_CI*, *TC_CCI*.

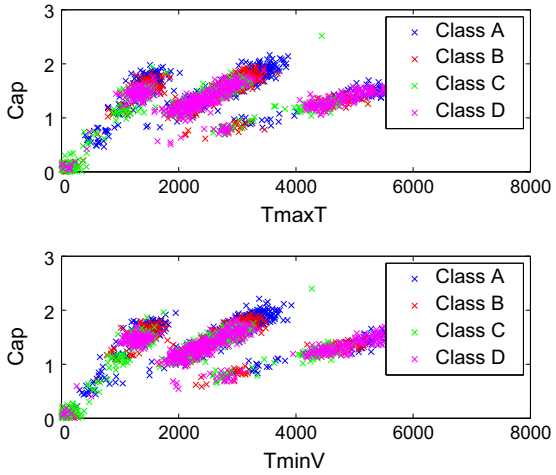

Fig. 3. Scatter plots displaying spread of battery parameters across classes. (a) *Cap* v/s t_{maxT} and (b) *Cap* v/s t_{minV}.

In Eq. (17), $\lambda_{i,j}$ is a distance between the data points and the support vectors. σ is the standard deviation in the data, and is treated as a fitting parameter. As mentioned earlier, the present study considers multiple features extracted from the data set as the input variable. Hence the x_i and x_j are vectors, and a scalar distance defined by:

$$\lambda_{i,j}^2 = \sum_{i,j}(x_i - x_j)^2 \tag{18}$$

is used in Eq. (17).

4. Results and discussion

In this section the performance–accuracy values as well as simulation time – of classification and regression models is investigated. The Section 4.1 discusses the accuracy statistics of the models along with computation time on a set of batteries. Sections 4.2–4.5 discusses the adaptability of these models across wide range of batteries; ranging from single battery to a set of batteries operated in diverse load and environment conditions. The overall approach of estimating RUL of an unknown battery is given in Fig. 1b.

4.1. Case 1: Multiple battery data

In the first case study, effectiveness of the proposed method for RUL estimation is demonstrated for a set of three batteries (B0033, B0034 and B0036). As can be observed from Table 1, these batteries have same EOL condition, operating temperature and number of cycle, however, their discharge current and end voltage are different. The purpose of this case study is to evaluate performance of the proposed method on a set of batteries that have similar operating characteristics but each battery has its own independent signature. This methodology helps in understanding the applicability of proposed method as a generic tool that can suit any of the batteries. The evaluation of accuracy of both the stages-classification and regression-are done separately, however the overall time-complexity of the approach is measured to check its applicability in real-time scenarios.

For classification purpose, all the discharge cycles from three batteries are aggregated. The aggregated data constitutes 591 cycles, 70% of this data is considered for classification model training (414 cycles) and rest for model testing (177 cycles). To ensure

tarjomehrooz.com 0902 795 28 76 ترجمه تخصصی توسط دکتری رشته مربوطه و برای کلیه زبان های خارجی + شبیه سازی مقالات با کلیه نرم افزار ها متلب گمز و ...

Table 2
Class-level accuracy of the classification model.

Class	TP rate	FP rate	Precision	Recall	*F*-measure	ROC area
A	0.957	0.023	0.936	0.957	0.946	0.967
B	0.933	0.023	0.933	0.933	0.933	0.955
C	0.833	0.037	0.875	0.833	0.854	0.898
D	0.909	0.038	0.889	0.909	0.899	0.936
Wt. avg.	0.91	0.03	0.909	0.91	0.909	0.94

TP: true positive.
FP: false positive.

an unbiased sample, the testing and training dataset is created using a random number generator. Training dataset consists of 101 cycles representing class A, 105 cycles representing class B, 105 cycles representing class C and 103 cycles representing class D. Classification model is created using SVM classifier with '*Radial Basis Function*' as the kernel. During training phase, parameters are optimized and final optimized parameter list is derived to create a robust model. Features selected for final training after optimization are *VCE* and *VC_FI*.

The model with the above mentioned 2 parameters is tested with the 30% of the data (177 cycles). The model correctly classifies 161 out of 177 cycles; thus the resultant classification accuracy is **94.15**%. The root mean squared error for classification is 0.2126 with Kappa statistic of 0.8794. Table 2 provides detailed classification accuracy for each class along with other statistical parameters and Table 3 provides the confusion matrix of the classification.

The regression model is built using the class D cycle data from the dataset of 3 batteries. This model is built using 103 (70% of data) cycle data and remaining 44 cycles are used to test the model. The regression model is built using SVR code developed in MATLAB. Based on the classification exercise, *VCE* and *VC_FI* are the inputs to the SVR and RUL is the output. In Fig. 4, the regression model prediction is compared against the training and testing data. The root mean squared error for the test data is 0.2420%, thus the resultant prediction accuracy is >**99**%. The results for the model comparison with the data used in the training phase are shown in Fig. 4a, and the % error, defined as $\left(1-\frac{\mathrm{RUL}_{data}}{\mathrm{RUL}_{model}}\right)*100$ is shown in Fig. 4b. The corresponding results for the test data are shown in Fig. 4c and d. In Fig. 4b and d, the value of the error at 95% confidence interval is marked as the horizontal lines. The root mean squared error (RMSE), the values of the lower bound (LB) and upper bound (UB) for this case are given in Table 4. The figure shows that the model can estimate RUL with minimal error irrespective of the battery cycle.

Table 3
Confusion matrix. Bold values indicate correctly classified samples.

Class	Classified as			
	A	B	C	D
Case 1				
A	**44**	2	0	0
B	0	**42**	3	0
C	1	1	**35**	5
D	2	0	2	**40**
Case 2				
A	**13**	0	0	0
B	0	**12**	0	0
C	1	0	**15**	1
D	0	0	0	**17**
Case 3				
A	**21**	0	0	0
B	4	**16**	1	0
C	0	3	**19**	0
D	0	0	1	**16**
Case 4				
A	**86**	6	0	0
B	5	**84**	3	1
C	2	3	**77**	10
D	1	0	6	**85**
Case 5				
A	**146**	12	0	4
B	13	**123**	25	1
C	4	16	**122**	20
D	4	1	22	**135**

A distinct feature of the model is extremely low errors for the training set. The training and testing data sets do not have any elements in common. Under these conditions, it is to be noted that the 95% of the data points of all the 3 batteries predicted by the model are within a reasonable error bounds. To establish computational efficiency of the proposed method, execution time of the MATLAB implementation on a desktop system (Intel i3 3.2 GHz dual core processor, 4.0 GB RAM, 32-bit Microsoft Windows 7) is investigated. The computation time for RUL estimation of a battery with 196 discharge cycles is **1.26** ms. This time includes the time taken by feature computation, classification and regression modules.

4.1.1. Case 1A: RUL Prediction of an untested battery

To investigate accuracy of the regression model to predict RUL of a kind of a battery different from the batteries used for training, the model is trained using the class D cycle data from batteries B0033, B0036 and tested for the battery B0034. The features selected for training are *VCE* and *VC_FI*. The regression model outcome for testing and training data is shown in Fig. 5a–d and the detailed statistics is provided in Table 4. The prediction RMSE for testing data is 0.11%, making it an efficient model with average accuracy of 99.89% for RUL prediction of new kind of batteries.

4.1.2. Case 1B: Effect of SVM classification error

In a multi-step approach, accuracy of initial steps is expected to impact the accuracy of subsequent steps. In a proposed two step approach, misclassification in a SVM step, where a battery belonging to different class is erroneously classified as class D, may impact RUL prediction accuracy of the SVR. To investigate the effect of SVM classification error on the RUL prediction accuracy, the regression model is trained using the class D data and tested for a randomly selected mixture of class C and class D data. For the present test case, the regression model is trained and tested for the battery B0034. Similar to the previous test cases, *VCE* and *VC_FI* are used as features for training. RUL prediction accuracy of the regression model for testing and training data is shown in Fig. 6a–d and the detailed statistics is provided in Table 4. The prediction RMSE for testing data is 0.21% while the maximum RUL prediction error is about 6%. The proposed multi-step approach, thus, ensures high RUL prediction accuracy even in view of the erroneous classifier output. It should be noted that the SVM classification error primarily results in a conservative estimate of the RUL, thus, safe battery operation is ensured even in view of the erroneous SVM classification.

4.1.3. Prognostic horizon of multi-step approach

In the proposed approach the SVM and SVR are trained offline and subsequently used online for RUL prediction. The predicted RUL is expected to aid in the prognostic task of the BMS. In this paper, the prognostic capability of the proposed multi-step approach is demonstrated using *Prognostic Horizon*, which is a widely used metric for comparing prognostic algorithms [59]. For this test case, class D data from batteries B0033 and B0036 is used for training the SVR and the data from battery B0034 is used for testing. The SVR is trained using *VCI* and *VC_FI* as features. To account for the SVM classification error, 20% data belonging to

tarjomehrooz.com 0902 795 28 76 ترجمه تخصصی توسط دکتری رشته مربوطه و برای کلیه زبان های خارجی + شبیه سازی مقالات با کلیه نرم افزار ها مثلب گمز و...

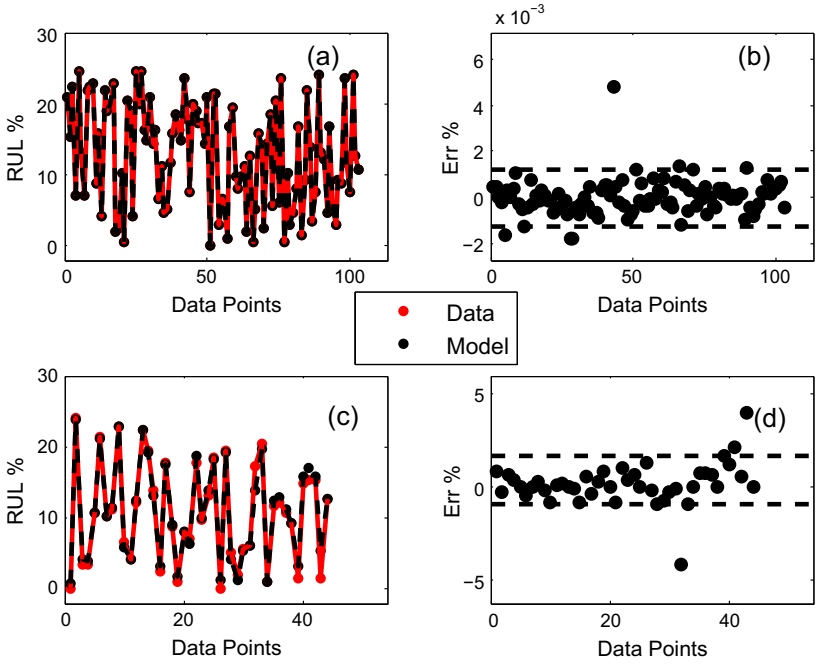

Fig. 4. (a) Comparison of estimated RUL% estimated by regression model with data, for the training set that includes B0033, B0034 and B0036. (b) Error in RUL% estimation by regression model with data for the training set. The 95% confidence intervals are also shown. (c) Comparison of estimated RUL% estimated by regression model with data for the testing set. (d) Error in RUL% estimation by regression model with data, for the testing set. The 95% confidence intervals are also shown.

Table 4
Statistical analysis of test cases.

	RMSE	95% LB	95% UB
Case 1			
Training set	6e−7	−0.0013	0.0012
Testing set	0.1659	−0.8882	1.6534
Case 1A			
Training set	3e−7	−0.0011	0.001
Testing set	0.11	−1.85	0.96
Case 1B			
Training set	1.032e−7	−0.00048	0.000494
Testing set	0.21175	−4.787	0.1553
Case 2			
Training set	2.85e−7	−0.00087	0.00112
Testing set	0.3582	−0.699	1.5007
Case 3			
Training set	0.0004	−0.0310	0.0352
Testing set	0.8681	−7.4849	5.7270
Case 4			
Training set	0.0005	−0.0546	0.0415
Testing set	0.3766	−7.0381	8.1358
Case 5			
Error (in%)	RMSE	95% LB	95% UB
Training set	7.32e−06	−0.00495	0.00465
Testing set	0.4125	−7.986	7.1393
Case 6			
Training set	0.0026	−0.09909	0.0729
Testing set	0.357	−10.75	7.87

class C is also used for testing. In Fig. 7, the predicted RUL is compared with the true RUL. Prognostic horizon for the test case is also shown in the figure. The desired RUL prediction accuracy is given in terms of $\pm\alpha$ bound, where $\alpha = 2$ is used in the present test case. The shaded region in the figure shows the desired RUL prediction accuracy. The prognostic horizon is given by the time between the algorithm first achieves a desirable accuracy to the battery end of life. The proposed algorithm has a prognostic horizon of about 50 cycles for the present test case, and accurately predicts the RUL when about 25% of the useful life of the battery is remaining.

4.2. Case 2: Single battery data

The RUL estimation model presented in this paper is tuned for a particular battery and its performance is evaluated. To create this model complete discharge cycle data from the battery B0036 is considered. Classification model is built using 70% of 197 cycles and tested for the remaining 59 cycles. Following the parameter optimization, *VCE* and *VC_FI* are identified as critical parameters and used for classification and regression model building. The classification model correctly classifies 57 out of 59 cycles, representing **96.61**% accuracy and kappa of 0.9545. Table 3 provides the confusion matrix for this model.

The corresponding regression model is built using class D cycles of battery B0036. There are total of 49 cycles belonging to class D, out of which 70% of cycles are randomly picked for training purpose and rest are used for testing the regression model using the MLP kernel. The testing outcome shows that model has very low error (RMSE) of 0.16554% while testing, making it an efficient model with average accuracy of 99.80%. Fig. 8a–d shows the regression model outcome for training and test data and the detailed statistics is provided in Table 4. It can be seen that this model has very good classification as well as regression accuracy; hence can be readily used for batteries operating in same environment as B0036.

4.3. Case 3: Two batteries at various temperatures

The next experiment is performed on data created by combining discharge cycles of B0005 and B0056. As can be noted from Table 1, these batteries are tested with the same discharge parameters; however, the operating temperature of the batteries is different. B0005 is tested at an ambient temperature of 24 °C whereas B0056 is tested at 4 °C.

tarjomehrooz.com 0902 795 28 76 ترجمه تخصصی توسط دکتری رشته مربوطه و برای کلیه زبان های خارجی + شبیه سازی مقالات با کلیه نرم افزار ها مثلب گمز و ...

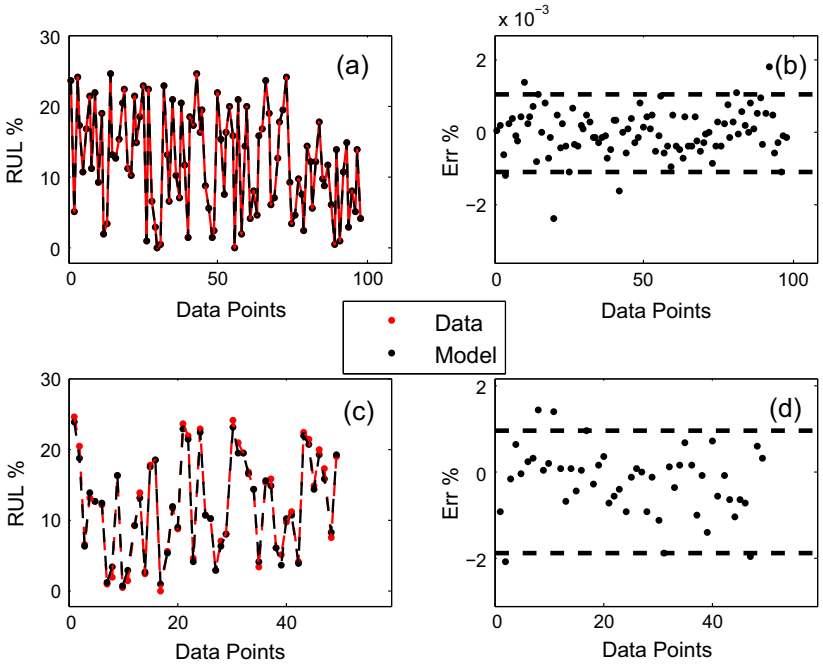

Fig. 5. Figure shows regression model outcome trained using data from batteries B0033, B0036 and tested for the battery B0034. The figures a–d represents the corresponding results as Fig. 4. In (a and c) of this figure, estimated RUL% value is represented in black color and experimental data in red color. (For interpretation of the references to colour in this figure legend, the reader is referred to the web version of this article.)

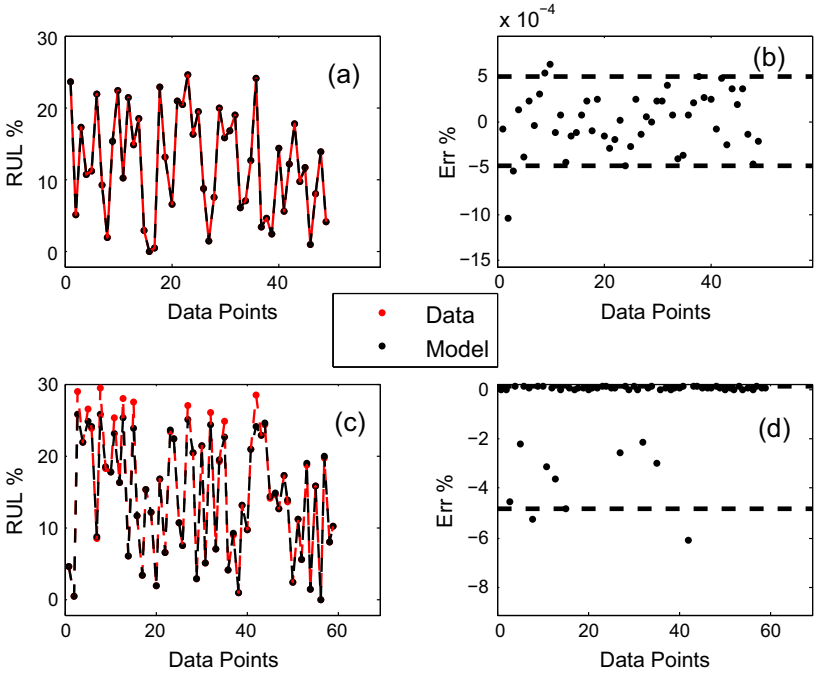

Fig. 6. Figure shows regression model outcome when SVM classifier erroneously classifies class C data as class D. For the test case, class D data of the battery B0034 is used for training and randomly selected 20% data from class C is used for testing. The figures a–d represents the corresponding results as Fig. 4. In a, c of this figure, estimated RUL% value is represented in black color and experimental data in red color. (For interpretation of the references to colour in this figure legend, the reader is referred to the web version of this article.)

Classification model is created using 70% of total discharge cycles, i.e. out of 270 cycles 189 cycles are used for model training and remaining 81 cycles are used for model testing. 270 cycles are divided almost equally across classes; classes A, C having 68 cycles and classes B and D having 67 cycles. Model feature vectors are optimized and finally two features, *VCE*, and *VC_FI* are used. Model parameters are set to same value as mentioned in Section 4.1. The model correctly classifies 72 cycles (**88.88**%) with kappa of 0.8513. Table 3 provides the confusion matrix for this model.

Regression model is built using 47 cycles of class D data (70%). This model is built using the same input parameters defined above, *VCE* and *VC_FI*. The model is tested using remaining 20 cycles of data. The testing and training datasets are mutually exclusive and are randomly selected. This model has RMSE of 0.86% on

tarjomehrooz.com 0902 795 28 76 ترجمه تخصصی توسط دکتری رشته مربوطه و برای کلیه زبان های خارجی + شبیه سازی مقالات با کلیه نرم افزار ها مثلب گمز و ...

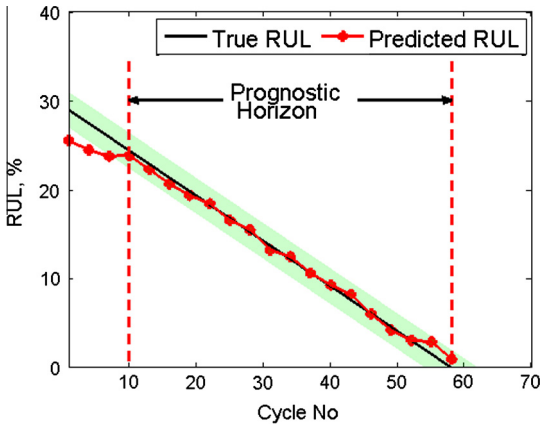

Fig. 7. Figure shows prognostic horizon of the proposed approach.

testing (results not shown), resulting in average accuracy of 99%. The 95% bounds on under and over estimation error are given in Table 4.

From the results, it can be observed that model performance is low compared to single battery case. It is interesting to note that the accuracy is also lower than 3 battery case discussed in Section 4.1. It is a well-known fact that batteries operated at different temperature ranges behave differently. Hence it can be seen that the model described in this work is able to distinguish such changes due to operating conditions as well. It is also important for designer to choose right set of batteries for combining and training models.

4.4. Case 4, 5: Multi-battery data at high and low temperatures (HT/LT)

This experiment is carried out to check performance of the proposed approach on a set of batteries operated at a similar operating temperature, but with totally different operating profiles. From Table 1, nine batteries are chosen that have operating temperature of 24 °C or 44 °C for the study at HT. For the LT studies, the data of 10 batteries at 4 °C were chosen.

To build classification model at HT, discharge cycle data from the nine batteries is aggregated, which makes total number of data point as 1236. Data splitting for testing and training is carried out in same way as mentioned earlier. For training, total 867 cycles are used comprising of 217 cycles from class A, 219 cycles from class B, 214 cycles from class C and 217 cycles from class D. In this experiment too, SVM classifier with '*Radial Bases Function*' is used to build the classifier model. The features selected after parameter optimizations are *VCE*, and *VC_FI*. The classification accuracy for this test case is **89.97**% with kappa value of 0.8663 and *RMSE* of 0.2239. Table 3 provides confusion matrix for the tested cycles. Regression model is built using 216 discharge cycles belonging to class D and rest 93 (30%) cycles are used to test the model. Model is built using the same 2 features as defined above, and MLP kernel is used. Fig. 9 shows comparison of the model with respect to experimental data, and the accuracy values are given in Table 4. The regression model for HT scenario has a RMSE of 0.3766. The 95% over and under estimation errors are at 8.13 and 7.04 percentage. As mentioned earlier, the accuracy is much higher for the training set.

In a similar manner, the model is tested at LT case, and the results are seen in Fig. 10. For this experiment all the batteries that operate with an ambient temperature of 4 °C are chosen. After classification the total data set is 231 cycles. Regression model is built using 162 of these data, and the model is tested using 69 discharge cycles belonging to class D. Model is built using the same parameters and kernel as discussed above. For the LT case, the accuracy (Table 4) is in the same range as the HT, demonstrating that the model can be used with equal confidence across temperatures.

4.5. Case 6: All battery data

Purpose for this experiment is to check generalizability of the model on a given set of diverse data. Hence to carry out this experiment discharge cycle data from all 19 batteries are aggregated. Total data available after aggregation is 2166 cycles. To build the

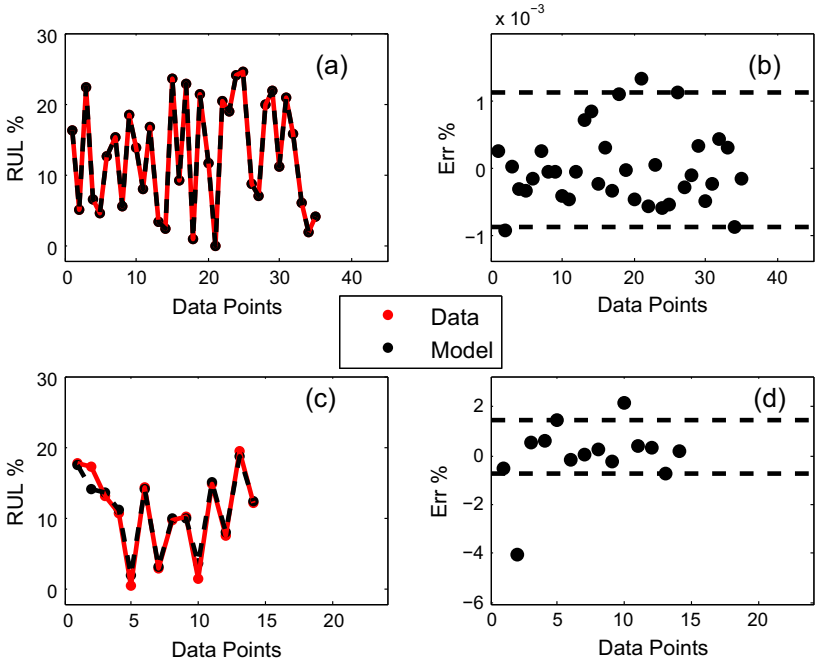

Fig. 8. (a–d) Figure shows single battery (B0036) regression model outcome. The figures a–d represents the corresponding results as Fig. 4. In a, c of this figure, estimated RUL % value is represented in black color and experimental data in red color. (For interpretation of the references to colour in this figure legend, the reader is referred to the web version of this article.)

tarjomehrooz.com 0902 795 28 76 ترجمه تخصصی توسط دکتری رشته مربوطه و برای کلیه زبان های خارجی + شبیه سازی مقالات با کلیه نرم افزار ها مثلب گمز و...

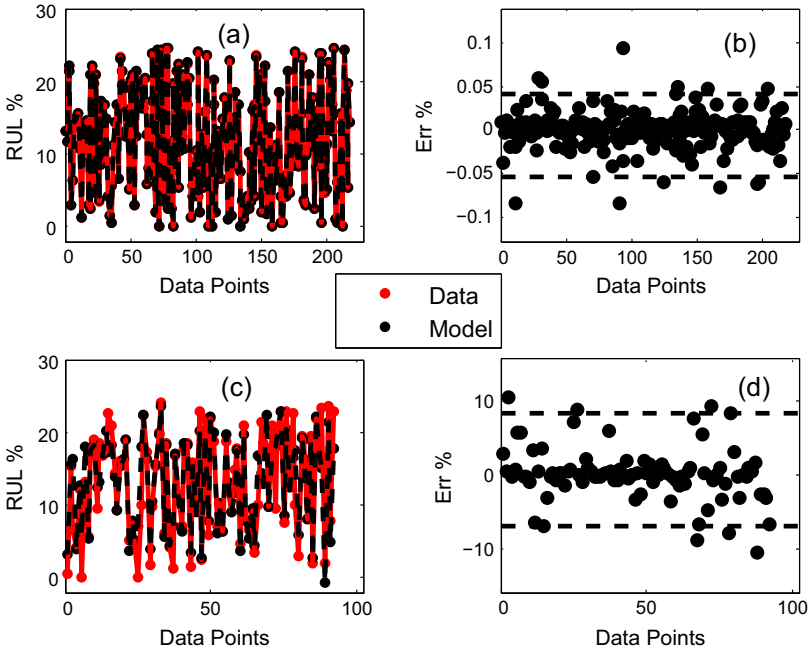

Fig. 9. (a–d) Graph displaying regression outcome for multi-battery same temperature case (HT). In a, c the estimated RUL% value is represented in black color and experimental data in red color. (For interpretation of the references to colour in this figure legend, the reader is referred to the web version of this article.)

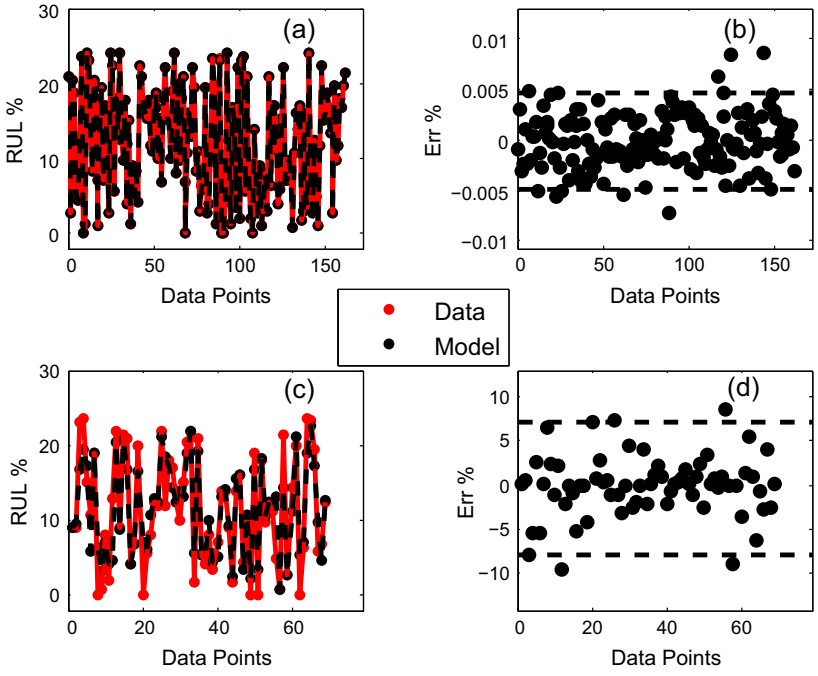

Fig. 10. (a–d) Graph displaying regression outcome for multi-battery same temperature case (LT). In a, c estimated RUL% value is represented in black color and experimental data in red color. (For interpretation of the references to colour in this figure legend, the reader is referred to the web version of this article.)

classification model, the complete data is split into training (70%) and testing (30%) data. Training dataset of 1518 cycle is composed of 381 cycles from class A, 382 cycles representing class B, 377 cycles representing class C and 378 cycles representing class D. Testing data (648 cycles) has equal representation of 162 cycles from each class. In this experiment also same classifier parameters are used as described in previous experiments. The critical features selected for final training after optimization are *VCE*, and *VC_FI*.

The classification model can correctly classify 526 cycles out of 648 cycles – the accuracy of classification is **81.17**%. RMSE of this model is 0.3068 with better Kappa value of 0.749. Table 3 provides confusion matrix. To build regression model 540 discharge cycles belonging to class D are chosen. 70% of this data (378 cycles) is used for regression model training and remaining 30% of data (162 cycles) is used for testing the model. Model is built using the above mentioned features and *SVR* with MLP kernel is used

tarjomehrooz.com 0902 795 28 76 ترجمه تخصصی توسط دکتری رشته مربوطه و برای کلیه زبان های خارجی + شبیه سازی مقالات با کلیه نرم افزار ها مثلب گمز و ...

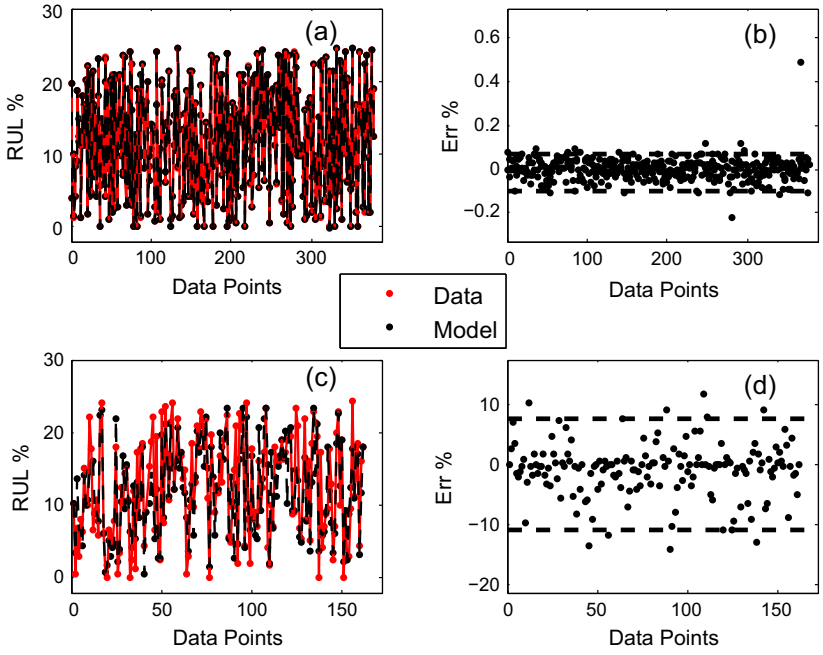

Fig. 11. (a–d) Graph displaying outcome of all battery regression model. In a, c the estimated RUL% value is represented in black color and experimental data in red color. (For interpretation of the references to colour in this figure legend, the reader is referred to the web version of this article.)

to build the regression model. The model performance against the experimental data is shown in Fig. 11.

This model has a RMSE of 0.357%, with 95% over and under estimation error of 7.87% and 10.75% (Table 4). The models built in this experiment have larger errors compared to the ones discussed in previous scenarios. This level of performance is justifiable as the input data is diverse in all directions of measurement. The average accuracy of both classification and regression models although are comparable with existing literature, it should be noted that this experiment involves multi-battery data. Hence this kind of generic models can be used for the batteries whose past operating history is unknown. It is also interesting to observe that cycling data of multiple batteries can be represented in terms of only 2 critical feature vectors. The accuracy can be enhanced further by training the model with larger datasets.

4.6. Model limitations and future work

The multi-step model proposed in this paper is extensively tested across a set of batteries to demonstrate accuracy. In the future, authors will investigate the accuracy of the multi-step approach for RUL prediction of batteries cycled using continuously changing load profiles, like UDDS and HPPC drive cycles. Being a data-driven approach, accuracy of the multi-step model depends on the data availability in the testing region. Multilayer frameworks for a SVM and SCR can be investigated for improved prediction accuracy of the model with limited training data set. In the present implementation, the model is trained offline, which is subsequently used online for RUL estimation. In the future, active online learning algorithms can be investigated such that the multi-step approach can adaptively learn online whenever new data is available.

5. Concluding remarks

A novel data-driven method for Li-ion battery RUL estimation is presented in this work. The proposed approach uses a combination of classification and regression stages to develop an efficient RUL estimation algorithm which is amenable for on-board implementation. Effectiveness of the algorithm is demonstrated using a publically available cell cycling data. A minimal set of critical features are extracted from the battery data set, and is used as the input to the classification and regression models. The multistage method, in addition to increasing the accuracy and reduction in simulation time, also enables accurate RUL estimation of multiple batteries simultaneously and hence is generic in nature. The model is tested for various case scenarios, for batteries at varying temperatures and operating conditions with sufficient accuracy.

From the model performance for the case studies presented in the earlier sections, it can be concluded that this approach can be used as a potential on-board RUL estimation tool for EVs. Once the trained model is used online, from measured signals, the critical features can be estimated. Based on these critical features, a quick classification step can identify if the battery is near EOL. If that were the case, the regression model can subsequently estimate the accurate RUL, and this information can be indicated to the driver while the vehicle is in operation.

References

[1] Axsen J, Burke A, Kurani K. Batteries for plug-in hybrid electric vehicles (PHEVs): goals and the state of technology circa 2008. Tech Rep UCD-ITS RR-08e14, Institute of Transportation Studies, University of California Davis; 2008.
[2] Johansson B, Martensson A. Energy and environmental costs for electric vehicles using CO_2-neutral electricity in Sweden. Energy 2000;25:777–92.
[3] Hu X, Nikolce M, Johannesson L, Egardt B. Energy efficiency analysis of a series plug-in hybrid electric bus with different energy management strategies and battery sizes. Appl Energy 2013;111:1001–9.
[4] Tian Y, Xia B, Sun W, Xu Z, Zheng W. A modified model based state of charge estimation of power lithium-ion batteries using unscented Kalman filter. J Power Sources 2014;270:619–26.
[5] Rezvanizaniani SM, Liu Z, Chen Y, Lee J. Review and recent advances in battery health monitoring and prognostics technologies for electric vehicle (EV) safety and mobility. J Power Sources 2014;256:110–24.
[6] Kennedy B, Patterson D, Camilleri S. Use of lithium-ion batteries in electric vehicles. J Power Sources 2000;90:156–62.
[7] Hu X, Sun F, Yuan Z. Online model identification of lithium-ion battery for electric vehicles. J Central South Univ Technol 2011;18:1525–31.
[8] Pilleri S, Perrin M, Jossen A. Methods for state-of-charge determination and their applications. J Power Sources 2001;96:113–20.

tarjomehrooz.com 0902 795 28 76 ترجمه تخصصی توسط دکتری رشته مربوطه و برای کلیه زبان های خارجی + شبیه سازی مقالات با کلیه نرم افزار ها مثلب گمز و ...

[9] Lu L, Han X, Li J, Hua J, Ouyang M. A review on the key issues for lithium-ion battery management in electric vehicles. J Power Sources 2013;226:272–88.
[10] Nuhic A, Terzimehic T, Soczka-Guth T, Buchholz M, Dietmayer K. Health diagnosis and remaining useful life prognostics of lithium-ion batteries using data-driven methods. J Power Sources 2013;239:680–8.
[11] Chiang YH, Sean WY, Ke JC. Online estimation of internal resistance and open-circuit voltage of lithium-ion batteries in electric vehicles. J Power Sources 2011;196:3921–32.
[12] Plett GL. Extended Kalman filtering for battery management systems of LiPB-based HEV battery packs: Part 1 background. J Power Sources 2004;134:252–61.
[13] Plett GL. Extended Kalman filtering for battery management systems of LiPB-based HEV battery packs: Part 2 modeling and identification. J Power Sources 2004;134:262–76.
[14] Plett GL. Extended Kalman filtering for battery management systems of LiPB-based HEV battery packs: Part 3 state and parameter estimation. J Power Sources 2004;134:277–92.
[15] Hu C, Youn BD, Chung J. A multiscale framework with extended Kalman filter for lithium-ion battery SOC and capacity estimation. Appl Energy 2012;92:694–704.
[16] Xiong R, Sun F, Chen Z, He H. A data-driven multi-scale extended Kalman filtering based parameter and state estimation approach of lithium-ion polymer battery in electric vehicles. Appl Energy 2014;113:463–76.
[17] Lee SJ, Kim J, Lee J, Cho BH. State-of-charge and capacity estimation of lithium-ion battery using a new open-circuit voltage versus state-of-charge. J Power Sources 2008;185:1367–73.
[18] Bhangu BS, Bentley P, Stone DA, Bingham CM. Nonlinear observers for predicting state-of-charge and state-of-health of lead-acid batteries for hybrid-electric vehicles. IEEE Trans Vehic Technol 2005;54:783–94.
[19] Zou Y, Hu X, Ma H, Li SE. Combined state of charge and state of health estimation over lithium-ion battery cell cycle lifespan for electric vehicles. J Power Sources 2015;273:793–803.
[20] Xiong R, Sun F, Gong X, Gao C. A data-driven based adaptive state of charge estimator of lithium-ion polymer battery used in electric vehicles. Appl Energy 2014;113:1421–33.
[21] Marwe R. Sigma-point Kalman filters for probabilistic inference in dynamic state-space models. PhD thesis, Oregon Health and Science University; 2004.
[22] Plett GL. Sigma-point Kalman filtering for battery management systems of LiPB-based HEV battery packs Part 2: simultaneous state and parameter estimation. J Power Sources 2006;161:1369–84.
[23] Andre D, Appel C, Soczka-Guth T, Sauer D. Advanced mathematical methods of SOC and SOH estimation for lithium-ion batteries. J Power Sources 2013;224:20–7.
[24] Arulampalam MS, Maskell S, Gordon N, Clapp T. Tutorial on particle filters for online nonlinear/non-Gaussian Bayesian tracking. IEEE Trans Signal Proc 2002;50:174–88.
[25] Saha B, Goebel K. Modeling Li-ion battery capacity depletion in a particle filtering framework. In: Annual conference of the prognostics and health management society; 2009.
[26] Saha B, Goebel K, Poll S, Christophersen J. Prognostics methods for battery health monitoring using a Bayesian framework. IEEE Trans Inst Meas 2009;58:291–6.
[27] Olivares BE, Cerda Munoz MA. Particle-filtering-based prognosis framework for energy storage devices with a statistical characterization of state-of-health regeneration phenomena. IEEE Trans Instrum Meas 2013;62:364–76.
[28] Wang Y, Zhang C, Chen Z. A method for joint estimation of state-of-charge and available energy of $LiFePO_4$ batteries. Appl Energy 2014;135:81–7.
[29] Liu D, Luo Y, Liu J, Peng Y, Guo L, Pecht M. Lithium-ion battery remaining useful Life estimation based on fusion nonlinear degradation AR model and RPF algorithm. Neural Comp Appl 2014;25:557–72.
[30] Liu J, Wang W, Ma F. A regularized auxiliary particle filtering approach for system state estimation and battery life prediction. Smart Mater Struct 2011;20:1–9.
[31] Miao Q, Xie L, Cui H, Liang W, Pecht M. Remaining useful life prediction of lithium-ion battery with unscented particle filter technique. Microelectron Reliab 2013;53:805–10.
[32] Hu C, Jain G, Tamirisa P, Gorka T. Method for estimating capacity and predicting remaining useful life of lithium-ion battery. Appl Energy 2014;126:182–9.
[33] Saha B, Goebel K, Christophersen J. Comparison of prognostic algorithms for estimating remaining useful life of batteries. Trans Inst Meas Control 2009;31:293–308.
[34] Waag W, Fleischer C, Sauer DU. Critical review of the methods for monitoring of lithium-ion batteries in electric and hybrid vehicles. J Power Sources 2014;258:321–39.
[35] Bai G, Wang P, Hub C, Pecht M. A generic model-free approach for lithium-ion battery health management. Appl Energy 2014;135:247–60.
[36] Kang L, Zhao X, Ma J. A new neural network model for the state-of-charge estimation in the battery degradation process. Appl Energy 2014;121:20–7.
[37] Vapnik VN. The nature of statistical learning. Berlin: Springer-Verlag; 1995.
[38] Hansen T, Wang CJ. Support vector based battery state of charge estimator. J Power Sources 2005;141:351–8.
[39] Hu X, Sun F. Fuzzy clustering based multi-model support vector regression state of charge estimator for lithium-ion battery of electric vehicle. In: International conference on intelligent human–machine systems and cybernetics; 2009.
[40] Klass V, Behm M, Lindbergh G. Evaluating real-life performance of lithium-ion battery packs in electric vehicles. J Electrochem Soc 2012;159:A1856–60.
[41] Klass V, Behm M, Lindbergh G. A support vector machine-based state-of-health estimation method for lithium-ion batteries under electric vehicle operation. J Power Sources 2014;270:262–72.
[42] Dong H, Jin X, Lou Y, Wang C. Lithium-ion battery state of health monitoring and remaining useful life prediction based on support vector regression-particle filter. J Power Sources 2014;271:114–23.
[43] Saha B, Goebel K, Poll S, Christophersen J. Prognostics methods for battery health monitoring using a Bayesian framework. IEEE Trans Instrum Meas 2009;58:291–6.
[44] Wang D, Miao Q, Pecht M. Prognostics of lithium-ion batteries based on relevance vectors and a conditional three-parameter capacity degradation model. J Power Sources 2013;239:253–64.
[45] Andre D, Appel C, Soczka-Guth T, Sauer DU. Advanced mathematical methods of SOC and SOH estimation for lithium-ion batteries. J Power Sources 2013;224:20–7.
[46] Hu C, Jain G, Zhang P, Schmidt C, Gomadam P, Gorka T. Data-driven method based on particle swarm optimization and k-nearest neighbor regression for estimating capacity of lithium-ion battery. Appl Energy 2014;129:49–55.
[47] Liu D, Pang J, Zhou J, Peng Y, Pecht M. Prognostics for state of health estimation of lithium-ion batteries based on combination of Gaussian process functional regression. Microelectron Reliab 2013;53:832–9.
[48] Liu J, Wang W, Mac F, Yang YB, Yang CS. A data-model-fusion prognostic framework for dynamic system state forecasting. Eng Appl Artif Intell 2012;25:814–23.
[49] He H, Zhang Y, Xiong RC, Wang C. A novel Gaussian model based battery state estimation approach: state-of-energy. Appl Energy 2015;151:41–8.
[50] Hu X, Li SE, Jia Z, Egardt B. Enhanced sample entropy-based health management of Li-ion battery for electrified vehicles. Energy 2014;64:953–60.
[51] Widodo A, Shim MC, Caesarendra W, Yang BS. Intelligent prognostics for battery health monitoring based on sample entropy. Exp Sys Appl 2011;38:11763–9.
[52] Ng SSY, Xing Y, Tsui KL. A naive Bayes model for robust remaining useful life prediction of lithium-ion battery. Appl Energy 2014;118:114–23.
[53] Guo J, Lia Z, Pecht M. A Bayesian approach for Li-ion battery capacity fade modeling and cycles to failure prognostics. J Power Sources 2015;281:173–84.
[54] Lu C, Tao L, Fan H. Li-ion battery capacity estimation: a geometrical approach. J Power Sources 2014;261:141–7.
[55] Patil M, Krishnan SH. Automated real-time estimation of remaining useful life (RUL) of battery. Indian patent application no. 1024/CHE/2015.
[56] Saha B, Goebel K. Battery data set. NASA Ames Prognostics Data Repository; 2007. <http://ti.arc.nasa.gov/project/prognostic-data-repository>.
[57] Hall M, Frank E, Holmes G, Pfahringer B, Reutemann P, Witten IH. The WEKA data mining software: an update. SIGKDD Explorat 2009;11:10–8.
[58] Chang CC, Lin CK. LIBSVM: a library for support vector machines. ACM Trans Intell Syst Technol 2011;2:27.
[59] Saxena A, Celaya J, Saha B, Saha S, Goebel K. On applying the prognostic performance metrics. In: International conference on prognostics and health management; 2009.